

# Vismodegib Identified as a Novel COX-2 Inhibitor via Deep-Learning-Based Drug Repositioning and Molecular Docking Analysis

Muhammad Yasir, Jinyoung Park, Eun-Taek Han, Won Sun Park, Jin-Hee Han, Yong-Soo Kwon, Hee-Jae Lee, and Wanjoo Chun\*



Cite This: *ACS Omega* 2023, 8, 34160–34170



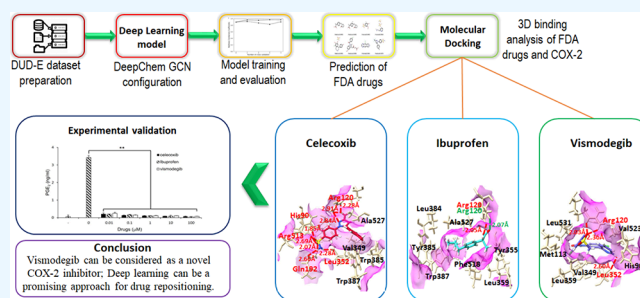
Read Online

ACCESS |

Metrics & More

Article Recommendations

**ABSTRACT:** Artificial intelligence algorithms have been increasingly applied in drug development due to their efficiency and effectiveness. Deep-learning-based drug repurposing can contribute to the identification of novel therapeutic applications for drugs with other indications. The current study used a trained deep-learning model to screen an FDA-approved drug library for novel COX-2 inhibitors. Reference COX-2 data sets, composed of active and decoy compounds, were obtained from the DUD-E database. To extract molecular features, compounds were subjected to RDKit, a cheminformatics toolkit. GraphConvMol, a graph convolutional network model from DeepChem, was applied to obtain a predictive model from the DUD-E data sets. Then, the COX-2 inhibitory potential of the FDA-approved drugs was predicted using the trained deep-learning model. Vismodegib, an anticancer agent that inhibits the hedgehog signaling pathway by binding to smoothened, was predicted to inhibit COX-2. Noticeably, some compounds that exhibit high potential from the prediction were known to be COX-2 inhibitors, indicating the prediction model's liability. To confirm the COX-2 inhibition activity of vismodegib, molecular docking was carried out with the reference compounds of the COX-2 inhibitor, celecoxib, and ibuprofen. Furthermore, the experimental examination of COX-2 inhibition was also carried out using a cell culture study. Results showed that vismodegib exhibited a highly comparable COX-2 inhibitory activity compared to celecoxib and ibuprofen. In conclusion, the deep-learning model can efficiently improve the virtual screening of drugs, and vismodegib can be used as a novel COX-2 inhibitor.



## INTRODUCTION

Drug repositioning is the process of finding new therapeutic applications for already approved drugs for other medical uses.<sup>1</sup> It can significantly expedite the drug development process, increase the value of existing drugs, and lead to new treatments for diseases that currently have no effective treatment options.<sup>2</sup> Accordingly, drug repositioning is becoming increasingly an important area of research in drug development.

Computer-aided drug design (CADD) has emerged as an increasingly valuable tool in the field of drug discovery and development.<sup>3</sup> Utilizing computational methods and software, CADD enables efficient screening of large compound libraries, offering a faster and more cost-effective alternative to traditional experimental approaches.<sup>4</sup> A key advantage of CADD is its ability to rapidly screen a large number of compounds, reducing the need for extensive laboratory testing, as in traditional experimental studies, which can be time-consuming and costly. By virtually screening a large number of compounds, CADD helps identify potential candidates for further synthesis and laboratory evaluation.<sup>5</sup>

Artificial intelligence is rapidly growing and holds immense potential to revolutionize the drug development process.<sup>6</sup> Deep learning (DL), which falls under the umbrella of artificial intelligence, allows DL models to learn from data and make predictions or decisions without the need for explicit programming.<sup>7</sup> DL is employed in drug development to examine extensive data sets including genetic and clinical information, enabling the identification of novel drug targets, accurate prediction of drug efficacy, and optimization of drug properties.<sup>8,9</sup> One of the primary benefits of DL in drug development is its ability to analyze large and complex data sets.<sup>10</sup> Traditional data analysis methods, such as manual inspection and statistical approaches, are often time-consuming and require substantial human effort. DL algorithms, on the other hand, can quickly and efficiently analyze large amounts of

**Received:** July 26, 2023

**Accepted:** August 24, 2023

**Published:** September 6, 2023



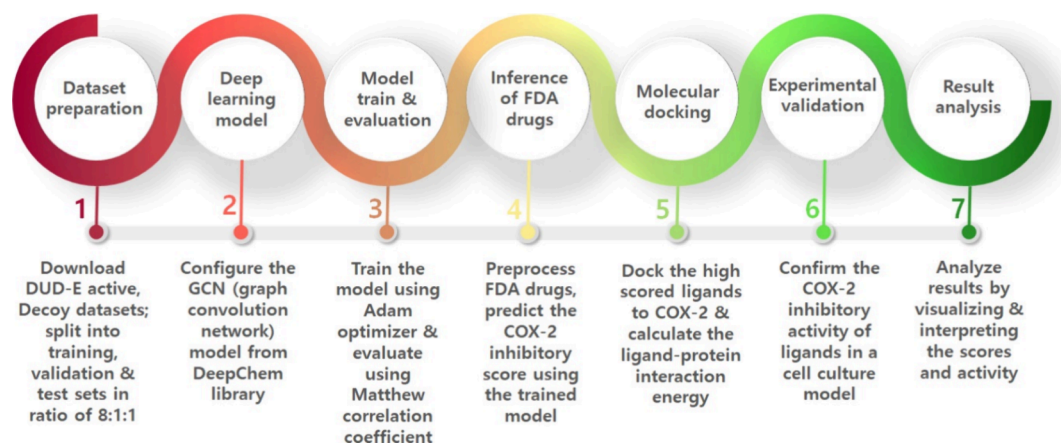


**Figure 1.** Workflow of combining deep-learning, molecular docking, and experimental evaluation approaches for drug repositioning of novel COX-2 inhibitors.

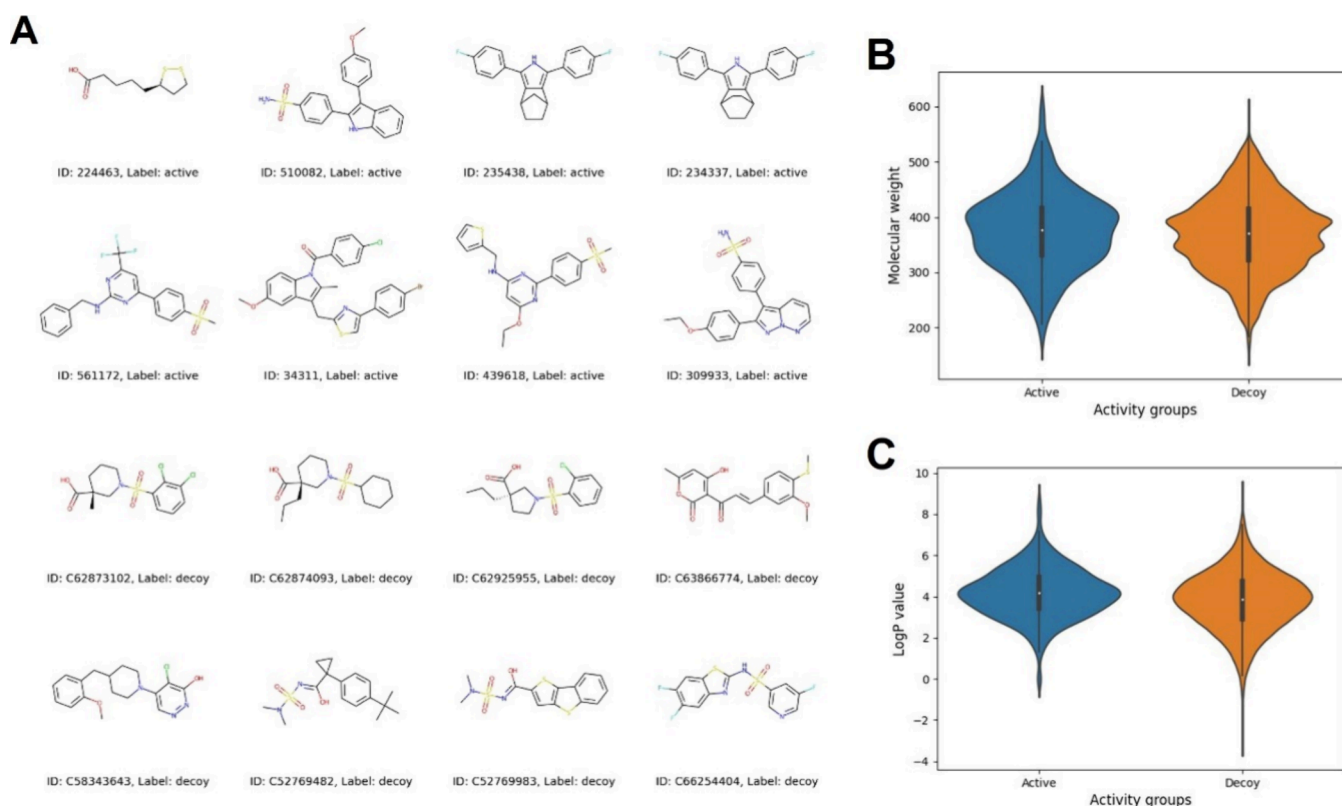


**Figure 2.** (A–C) Representative image of active and decoy compounds (A). Distribution of molecular weight (B) and LogP (C) values in active and decoy compounds.

data, identify patterns, and make predictions, greatly accelerating the drug development process.<sup>11</sup> Another benefit of DL in drug development is its ability to predict the effectiveness and toxicity of compounds.<sup>12</sup> Through the analysis of extensive data sets, DL algorithms can identify patterns that are indicative of drug efficacy and toxicity, allowing for the prediction of these properties prior to the synthesis and laboratory testing of the drug. Therefore, the application of DL in CADD can further significantly improve the speed, efficiency, and success of the drug discovery and development process, making it a valuable tool in modern drug discovery research.

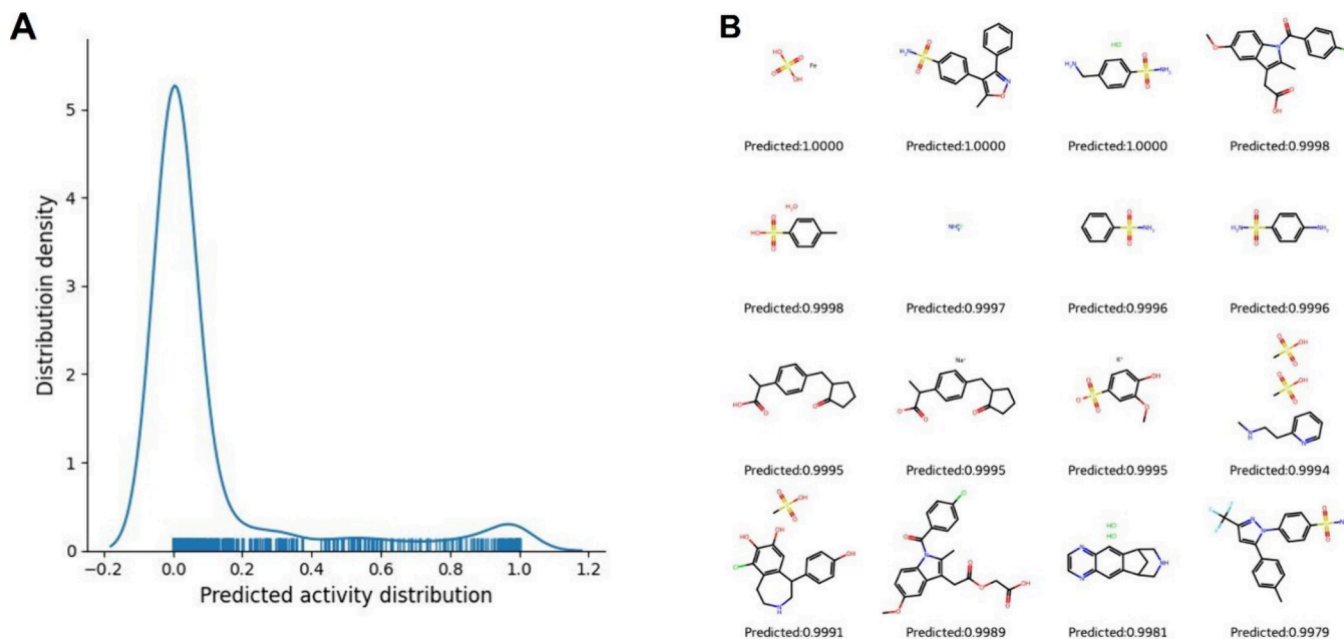
Cyclooxygenase 2 (COX-2), encoded by the prostaglandin-endoperoxide synthase 2 (PTGS2) gene, is an enzyme that is

involved in various physiological and pathological processes, such as inflammation and cancer. COX-2 catalyzes the conversion of arachidonic acid into prostanoids such as prostaglandins and thromboxanes. These prostanoids play important roles in a variety of pathologic conditions.<sup>13,14</sup> Diseases associated with aberrant activation of COX-2 include various inflammatory conditions such as rheumatoid arthritis and psoriasis. COX-2 has also been implicated in the development and progression of certain types of cancers, including colorectal, breast, and prostate cancer.<sup>15–17</sup> In addition, COX-2 has been associated with cardiovascular disease, Alzheimer's disease, and other conditions involving chronic inflammation.<sup>18,19</sup> Therefore, the present study focuses



**Table 1. Compounds That Were Mispredicted as False Negative (Active 1) and False Positive (Active 0) and Their Prediction Values**

neg	pos	active	SMILES
0.516292	0.483708	1	<chem>Clc4ccc(c3nn(c1cccc1)c2CCCCc23)cc4</chem>
0.617401	0.382599	1	<chem>FC(F)(F)S(=O)(=O)Nc1ccncc1Sc2cccc2</chem>
0.99782	0.00218	1	<chem>C[C@@]23C[C@H]1OC(=O)C(=C)[C@H]1C[C@H]2C(=C)C(=O)C=C3</chem>
0.859431	0.140569	1	<chem>OC(=O)c6ccc5OCc1cccc1\C(=C)\Cn3cnc4cc2OCOc2cc34)c5c6</chem>
0.996623	0.003377	1	<chem>Cc3ccc(Cl)c(Nc1cccc1c2nnc(NC#N)o2)c3Cl</chem>
0.816444	0.183556	1	<chem>OC(=O)c5ccc(OC/C=C/Cn4c(=O)n(Cc1cccc1)c(=O)n(Cc2cccc2)c3cccc3)c4=O)cc5</chem>
0.697728	0.302272	1	<chem>Cn3c(=O)oc4cc(c1 cm^3(C(F)(F)F)nn1c2ccc(Cl)cc2)ccc34</chem>
0.4373	0.5627	0	<chem>c1cc2c(cc1S(=O)(=O)N)[C@H]3C=CC[C@H]3[C@H](N2)c4cc(ccc4O)Br</chem>
0.499125	0.500876	0	<chem>O=C(O)C Oc1cccc1[C@H]1Nc2cccc2-c2nnc(SCc3ccc(Cl)cc3)nc2O1</chem>

**Figure 4.** (A, B) Distribution of GraphConvMol prediction (A) and structures (B) of highly predicted compounds from FDA-approved drugs.

sets in five cross-validations were 0.95 and 0.88, respectively (Figure 3A). Given that the MCC value of 1 indicates that all predictions are correct, the values of 0.95 and 0.88 indicate the robustness of the prediction model. It is usually acceptable that the MCC value of the test set is higher than that of the validation set because the model is trained on the training set and then validated on new and unseen data, which is a validation data set. In addition, the MCC value changes in five cross-validations indicated that the model is not overfitting over the training (Figure 3A). To evaluate the performance of the trained model on new and unseen data, a test set was subjected to the trained model to make predictions. As shown in Figure 3B, most decoy compounds were correctly predicted as inactive (less than 0.5 in predicted activity) with only a small fraction of compounds mispredicted as false positive. For active compounds in the test set, a majority of active compounds were correctly predicted as active (greater than 0.5 in predicted activity), with some compounds mispredicted as false negative (Figure 3B). Although there may not be a universal acceptance range for misprediction, it is generally desirable for a prediction model to minimize the number of false positives and false negatives. The numbers of false negatives and false positives are considered not significant in the present model. Compounds that were mispredicted as false negatives and false positives are summarized in Table 1. The

label in the active column indicates 1 (active) and 0 (decoy) in the test set, and values in neg and pos columns indicate the predicted activity of the compounds (Table 1).

**Prediction of COX-2 Inhibitory Potential from FDA-Approved Drugs.** The use of FDA-approved drugs for drug repositioning has several benefits. Since FDA-approved drugs have already gone through preclinical and clinical testing to determine their safety, dosing, and pharmacokinetics, the drug repositioning of FDA-approved drugs can have shorter timelines, lower development costs, and higher likelihood of success.

SMILES strings of FDA-approved drugs were subjected to the trained model with the GraphConvMol algorithm of DeepChem to predict the potential of the COX-2 inhibitory activity. The trained model predicted the COX-2 inhibitory activity of FDA-approved drugs in the range of 0 (no activity) to 1 (highly active). The majority of the compounds were predicted as inactive, whereas only small fractions of compounds were predicted as active (Figure 4A). Representative structures of compounds, which were predicted as highly active, were depicted with labels indicating their predicted values (Figure 4B).

Noticeably, the majority of the top-ranked compounds were known COX-2 inhibitors (Table 2), strongly indicating that the present model is highly robust and reliable. Celecoxib,

Table 2. Detailed Information on Drugs That Were Predicted with High COX-2 Inhibitory Potential

SMILES	neg	pos	drug name	target/action
<chem>Cc1ccc(-c2cc(C(F)(F)F)nn2-c2ccc(S(N)(=O)=O)cc2)cc1</chem>	0.0001	0.9999	celecoxib	selective COX-2 inhibitor
<chem>Nc1ccc(S(N)(=O)=O)cc1</chem>	0.0001	0.9999	sulfanilamide	sulfonamide antibacterial
<chem>Cc1ccc(-c2ncc(CI)cc2-c2ccc(S(C)(=O)=O)cc2)cn1</chem>	0.0003	0.9997	etoricoxib	selective COX-2 inhibitor
<chem>CS(=O)(=O)c1ccc(C(=O)Nc2ccc(Ct)(-c3cccn3)c2)c(CI)c1</chem>	0.0003	0.9997	vismodegib	hedgehog pathway inhibitor, anticancer
<chem>Cc1onc(-c2cccc2)c1-c1ccc(S(N)(=O)=O)cc1</chem>	0.0003	0.9997	valdecoxib	selective COX-2 inhibitor
<chem>NS(=O)(=O)c1ccc(C(=O)O)cc1</chem>	0.0008	0.9992	carzenide	antispasmodic
<chem>NS(=O)(=O)c1cccc1</chem>	0.0008	0.9992	benzenesulfonamide	antibacterial
<chem>COc1cc(S(=O)(=O)[O-])ccc1O.[K+]</chem>	0.0014	0.9986	potassium guaiacolsulfonate	expectorant
<chem>Cc1ccc(S(=O)(=O)O)cc1.O</chem>	0.0025	0.9975	p-toluenesulfonic acid monohydrate	catalyst
<chem>O=S(=O)(O)c1ccc2nc(-c3cccc3)[nH]c2c1</chem>	0.0028	0.9972	ensulizole	sunscreen agent
<chem>COc1ccc2c(c1)c(CC(=O)O)c(C)n2C(=O)c1ccc(CI)cc1</chem>	0.0036	0.9964	indomethacin	nonselective COX inhibitor
<chem>CC(C(=O)O)c1ccc(CC2CCCC2=O)cc1</chem>	0.0041	0.9958	loxoprofen	nonselective COX inhibitor
<chem>CC(C)Cc1ccc(C(C)C(=O)O)cc1</chem>	0.0057	0.9943	ibuprofen	nonselective COX inhibitor
<chem>CC(C(=O)O)c1cccc(C(=O)c2cccc2)c1</chem>	0.0067	0.9933	ketoprofen	nonselective COX inhibitor
<chem>CLNCc1ccc(S(N)(=O)=O)cc1</chem>	0.0076	0.9924	mafenide hydrochloride	antibacterial agent
<chem>CC(C(=O)O)c1ccc2c(c1)Cc1cccn1O2</chem>	0.0078	0.9922	pranoprofen	nonselective COX inhibitor
<chem>Cc1cc(C(C)(C)C)c(O)c(C(C)(C)C)c1</chem>	0.0110	0.9890	2,6-di-tert-butyl-4-methylphenol	antioxidant
<chem>CS(=O)(=O)Nc1ccc([N+](=O)[O-])cc1Oc1cccc1</chem>	0.0149	0.9851	nimesulide	selective COX-2 inhibitor
<chem>CCCCNc1cc(C(=O)O)cc(S(N)(=O)=O)c1Oc1cccc1</chem>	0.0153	0.9847	bumetanide	loop diuretic
<chem>O=S(=O)([O-])Oc1ccc(C(c2ccc(OS(=O)(=O)[O-])cc2)c2cccn2)cc1.[Na+].[Na+]</chem>	0.0192	0.9808	sodium picosulfate	laxative
<chem>Cc1c(C(=O)Nc2ccc(S(C)(=O)=O)cc2)cn(CCO)c1-c1cccc1C(F)(F)F</chem>	0.0239	0.9761	esaxerenone	antihypertensive
<chem>O=S(=O)(O)O.[Fe]</chem>	0.0261	0.9739	iron dextran	IV formulation of iron
<chem>O=C(O)C(O)C(O)C(=O)O</chem>	0.0262	0.9738	tartaric acid	antioxidant
<chem>CC(C(=O)O)c1ccc2c(c1)[nH]c1ccc(CI)cc12</chem>	0.0290	0.9710	carprofen	nonselective COX inhibitor
<chem>CC(C(=O)O)c1ccc(C(=O)c2cccs2)cc1</chem>	0.0329	0.9671	suprofen	nonselective COX inhibitor
<chem>Nc1c(CC(=O)[O-])cccc1C(=O)c1cccc1.O.[Na+]</chem>	0.0349	0.9651	amfenac sodium monohydrate	nonselective COX inhibitor
<chem>Cc1cccc1N1C(=O)c2cc(S(N)(=O)=O)c(CI)cc2NC1C[Cl-].[NH4+]</chem>	0.0404	0.9596	metolazone	thiazide-related diuretic
<chem>CCN(CC)CCNC(=O)c1cc(S(C)(=O)=O)ccc1OC.Cl</chem>	0.0441	0.9559	ammonium chloride	electrolyte
<chem>CCN(CC)CCNC(=O)c1cc(S(C)(=O)=O)ccc1OC.Cl</chem>	0.0447	0.9553	tiapride hydrochloride	neuroleptic and Huntington disease
<chem>Cc1cnc(NC(=O)C2=C(O)c3cccc3S(=O)(=O)N2C)s1</chem>	0.0457	0.9543	meloxicam	nonselective COX inhibitor

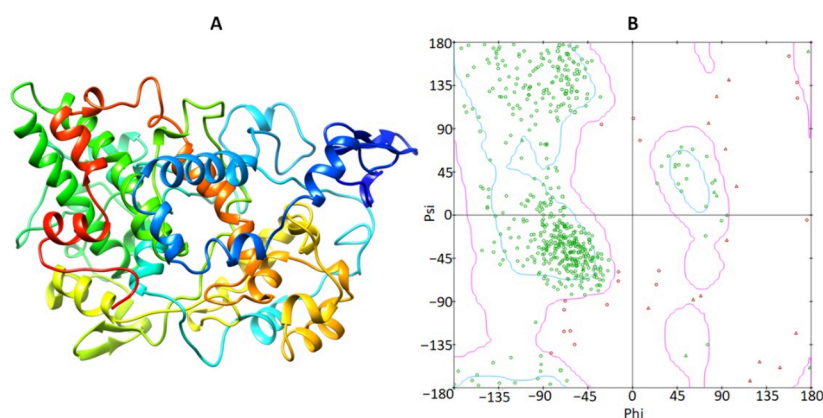
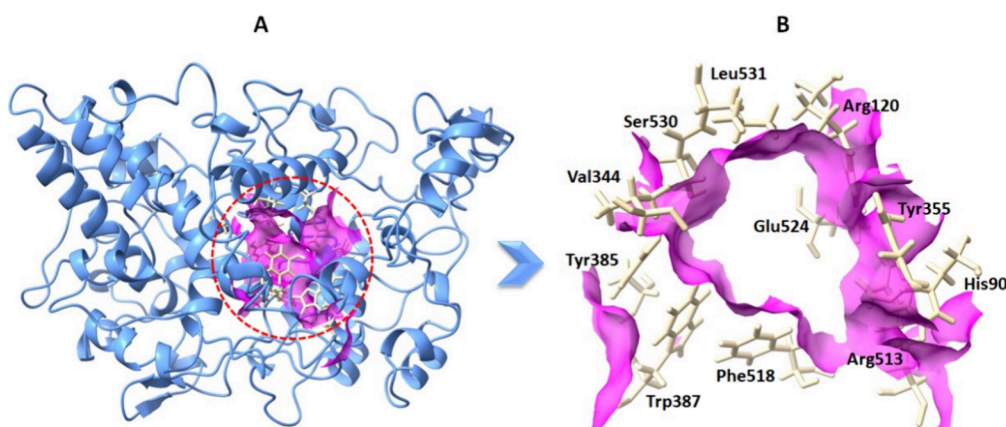


Figure 5. (A, B) 3D structure (A) of the COX-2 protein and the computed Ramachandran plot (B) of COX-2, calculated by Discovery Studio.

etoricoxib, and valdecoxib are selective COX-2 inhibitors and indomethacin, loxoprofen, ibuprofen, and ketoprofen are nonselective COX-2 inhibitors. Besides COX-2 inhibitors, some drugs with other medical indications were predicted as possible COX-2 inhibitors. One of the compounds with high potential is vismodegib, which is a medication used to treat basal cell carcinoma, a common type of skin cancer. It works by inhibiting a key signaling pathway in cells called the

hedgehog pathway, which is important for cell growth and division.<sup>27,28</sup> No association of COX-2 inhibition has been found in the literature search for vismodegib.

**Structural Analysis of the COX-2 Protein.** COX-2 belongs to the prostaglandin G/H synthase family and is known by several names including prostaglandin G/H synthase 2 (PGH2) and PTGS2.<sup>29</sup> It is made up of 311 amino acids forming a single chain (PDB ID: 5KIR). Loops,  $\alpha$ -helices, and



**Figure 6.** (A, B) Panel (A) manifests the binding pocket of COX-2. The whole protein is colored cornflower blue, while the binding surface area is colored magenta. Furthermore, the active site residues are mentioned on their position in the active region of the target protein and colored wheat (B).

$\beta$ -sheets occur in the overall protein structure (Figure 5A). Furthermore, a VADAR 1.8 structural study revealed that JAK2 is made up of 44%  $\alpha$ -helices, 11%  $\beta$ -sheets, 44% coils, and 26% turns. According to the Ramachandran plots, 92.7% of residues were in the allowed zone of dihedral angles phi ( $\varphi$ ) and psi ( $\psi$ ) (Figure 5B).

**Binding Pocket Analysis.** A binding pocket's function is determined by the collection of amino acid residues that surround it, in addition to its shape and location inside a protein.<sup>30</sup> The binding pocket residues of COX-2 were retrieved by employing the Discovery Studio ligand interaction approach and are mentioned as Val344, Tyr385, Trp387, Ser530, Phe518, Arg513, Glu524, Leu531, His90, Arg120, and Tyr355. Moreover, the binding pocket residues were verified from already published data.<sup>31</sup> Furthermore, the cocrystallized ligand was selected to define the binding sphere by the current selection approach. Therefore, the binding sphere values were adjusted as  $X = 22.9571$ ,  $Y = 1.0560$ ,  $Z = 34.0032$ , and the radius value was fixed as 8.2904 to study the interaction of selected compounds in the active region of COX-2 (Figure 6A,B).

**Molecular Docking Analysis.** All of the screened compounds that were docked against COX-2 were examined independently and scored based on the minimal docking energy and interaction energy values (Table 3). The CDocker module of Discovery Studio predicts to type of energy values (CDocker energy and CDocker interaction energy). CDocker energy exhibits the overall docking energy based on the ligand and protein 3D structural and physiochemical properties and CDocker interaction energy, which refers to the energy associated with the specific interactions between the ligand and the receptor. It quantifies the contribution of intermolecular interactions, such as van der Waals forces, electrostatic interactions, and hydrogen bonding, to the overall binding affinity. CDocker interaction energy provides insights into the strength and nature of the individual interactions between the ligand and the receptor.<sup>32,33</sup> Therefore, celecoxib demonstrates the lowest docking energy and interaction energy values. Moreover, ibuprofen and vismodegib came in the top 15 docked compounds. Although they exhibit high CDocker energy as compared to celecoxib, they exhibit highly negative interaction energy values (celecoxib, ibuprofen, and vismodegib manifest  $-47.8768$ ,  $-408083$ , and  $-39.646$ ), which demonstrate that although the overall docking energy was

**Table 3. Docking Energy Values (kcal/mol) of Screened Docked FDA Compounds against the COX-2 Protein, Calculated by Discovery Studio**

compounds	CDocker energy	CDocker interaction energy
celecoxib	22.86	47.88
bumetanide	32.06	46.16
etoricoxib	13.13	45.35
loxoprofen	26.27	43.94
ketoprofen	34.48	42.89
sodium picosulfate	-1.38	42.38
valdecoxib	13.34	42.26
tiapride hydrochloride	22.24	42.20
indomethacin	0.99	42.09
ibuprofen	36.95	40.81
amfenac sodium monohydrate	29.29	40.27
meloxicam	40.97	40.25
nimesulide	25.47	40.14
vismodegib	2.93	39.65
carprofen	26.34	39.28
pranoprofen	32.68	39.25
2,6-di- <i>tert</i> -butyl-4-methylphenol	24.07	36.92
suprofen	28.21	34.70
metolazone	14.53	33.64
2,3-dihydroxysuccinic Acid	27.11	32.22
carzenide, 4-sulfamoylbenzoic Acid	32.93	31.25
ensulizole	15.16	28.85
mafenide hydrochloride	28.03	27.22
potassium guaiacolsulfonate	16.60	24.65
esaxerenone	-17.71	23.01
sulfanilamide	24.05	22.06
Benzenesulfonamide	21.07	20.42
p-toluenesulfonic acid monohydrate	12.73	19.96
iron dextran	-37.01	8.51
ammonium chloride	2.63	2.64

high, they exhibit good interactions with the active region amino acids.

**Binding Interaction Analysis against COX-2.** Celecoxib, ibuprofen, and vismodegib docked against the COX-2 protein were further analyzed by Discovery Studio and UCSF

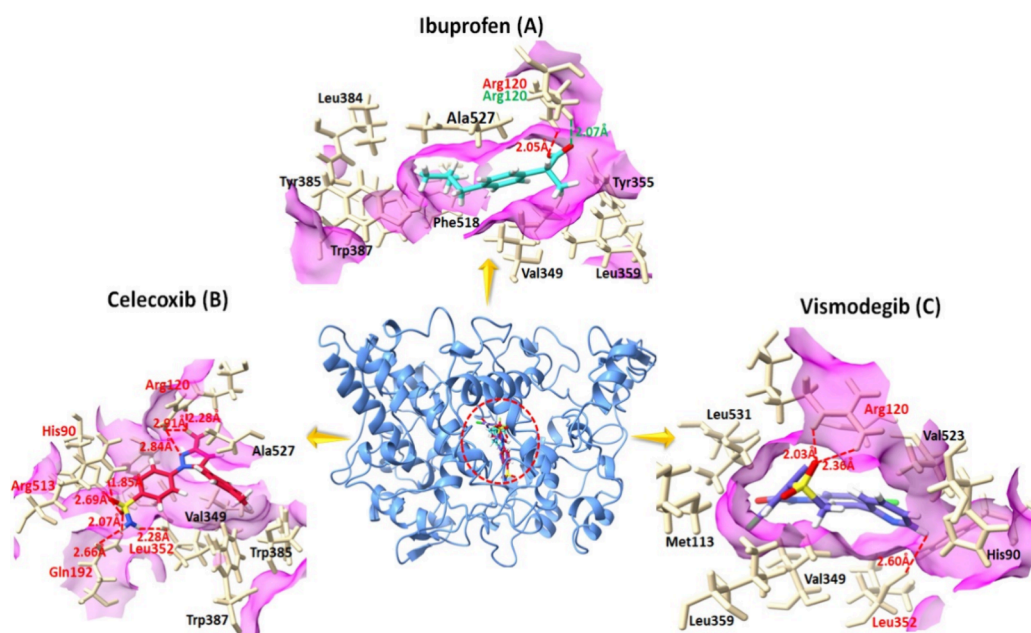


**Figure 7.** (A–C) Graphical representation of combine celecoxib, ibuprofen, and vismodegib interaction with the active region amino acid residues of COX-2. The whole structure of COX-2 is represented in the center (blue), while the interactions of ligands are predicted in three dimensions as A (ibuprofen), B (celecoxib), and C (vismodegib).

Chimera to examine and confirm the binding interaction with the active amino acid residues of COX-2.

**Ibuprofen.** The ligand–protein docking analysis of ibuprofen shows that the ligand binds within the active region of the target protein as shown in Figure 7A. The ibuprofen–COX-2 docked complex exhibits one hydrogen and one salt bridge. The oxygen atom of ibuprofen forms a hydrogen bond with Arg120 with a bonding distance of 2.05 Å. Additionally, another oxygen atom of ligand forms a salt bridge with the same Arg120 with a bond length of 2.07 Å.

**Celecoxib.** Celecoxib, which exhibits the lowest docking energy values in molecular docking studies, was confined in the active binding pocket of the COX-2 protein and formed eight hydrogen bonds with active region amino acid residues (Figure 7B). The celecoxib–COX-2 docked complex showed that one hydrogen atom of celecoxib formed two hydrogen bonds with Arg120 with bonding distance of 2.28 and 2.91 Å. Furthermore, a nitrogen atom of celecoxib form hydrogen bond with Arg513 with bonding distance of 2.69 Å. Moreover, another oxygen atom of ligand formed hydrogen bond with Arg120 with bond length of 2.84 Å. An oxygen atom of ligand formed hydrogen bond with Arg513 with bonding distance of 2.69 Å. Morevoer, another oxygen atom of compound form two hydrogen bonds with His90 and Gln192 with bond length of 1.85 and 2.07 Å, respectively. Additionally, two hydrogen atoms of celecoxib formed two hydrogen bonds with Gln192 and Leu352 with bonding distance of 2.66 and 2.28 Å, respectively.

**Vismodegib.** The ligand–protein docking analysis of vismodegib shows that ligands get docked within the active region of the target protein as shown in Figure 7C. The vismodegib–COX-2 docked complex forms three hydrogen bonds, which include the residues Arg120 and Leu352. The oxygen atom of vismodegib forms two hydrogen bonds with Arg120 with a bond length of 2.36 and 2.03 Å. Furthermore, the hydrogen atom of the ligand forms one hydrogen bond with Leu352 with a bonding distance of 2.60 Å.

Those interactions strongly suggest that the predicted drugs block the active region of COX-2 by hindering the active region amino acid residues.

**Experimental Validation.** Prostaglandin E<sub>2</sub> (PGE<sub>2</sub>) is a major prostaglandin produced by COX-2 in response to inflammatory stimuli. RBL-2H3 cells, a rat basophilic leukemia cell line, are commonly used in immunological research because the cells release histamine and other inflammatory mediators in response to various allergic stimuli.<sup>34</sup> We previously confirmed that COX-2 expression was significantly increased with the treatment of PMA and A23187 in RBL-2H3 cells.<sup>35</sup> To validate the results from the computational study, the inhibitory activity of the drugs (celecoxib, ibuprofen, and vismodegib) was examined by measuring the PGE<sub>2</sub> levels in PMA/A23187-challenged RBL-2H3 cells. The treatment of PMA/A23187 resulted in the considerable release of PGE<sub>2</sub> and all tested drugs significantly attenuated PGE<sub>2</sub> release from the cells, presumably inhibiting the enzyme activity of upregulated COX-2 in RBL-2H3 cells (Figure 8). Compared to known

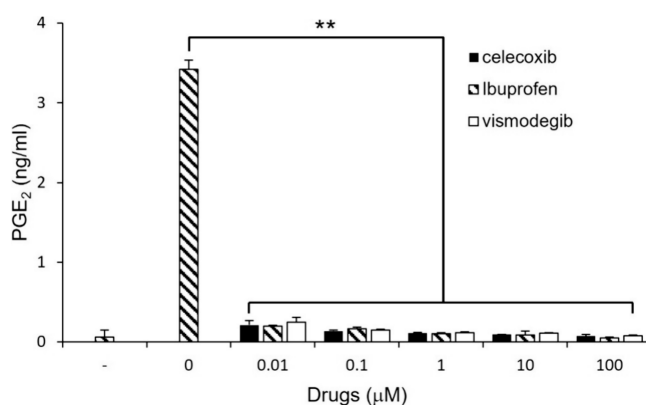


**Figure 8.** Inhibition of PMA/A23187-induced PGE<sub>2</sub> release in RBL-2H3 cells.

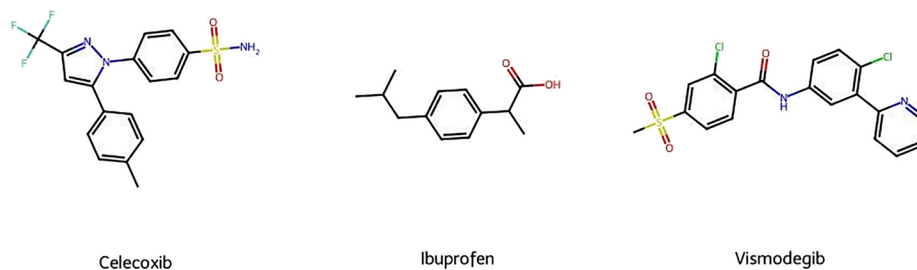


**Figure 9.** Structures of celecoxib, ibuprofen, and vismodegib.

COX-2 inhibitors such as celecoxib and ibuprofen, vismodegib exhibited quite potent COX-2 inhibitory activity. The result suggests that the strong COX-2 inhibitory activity of vismodegib, which is similar to these known inhibitors, indicates its potential usage as a novel COX-2 inhibitor. However, vismodegib, which is a hedgehog-signal inhibiting anticancer agent to treat advanced basal cell carcinoma, a type of skin cancer, has notable adverse effects including alopecia, muscle spasms, and dysgeusia.<sup>36</sup> Therefore, using vismodegib as an antiallergic medication that inhibits COX-2 would require caution.

#### Structural Evaluation and Similarity Comparison.

Several top-ranked drugs in the COX-2 inhibitory potential prediction share common structural moieties. Celecoxib and sulfanilamide contain the sulfonamide group, while rofecoxib, etoricoxib, and vismodegib share the sulfone group (Figure 9). The result indicates that these structural motifs might play a role in the binding of drugs to the active site of COX-2. However, other structural motifs might also contribute to the binding of the drugs to COX-2. Ibuprofen, ioxoprofen, and ketoprofen are classified as propionic acid derivatives, while indomethacin belongs to the indol acetic acid family. Although the drugs share some structural moieties, their overall similarity was not significant when calculated with Tanimoto similarity (Table 4).

**Table 4.** Tanimoto Similarity Comparison of Celecoxib, Ibuprofen, and Vismodegib

similarity	celecoxib	ibuprofen	vismodegib
celecoxib		0.121212	0.258621
ibuprofen	0.121212		0.138614
vismodegib	0.258621	0.138614	

## CONCLUSIONS

As drug development becomes a longer and more costly process, it is crucial to explore emerging techniques that can enhance it. Utilizing artificial intelligence has proven to be a rapid and highly productive method for identifying potential novel compounds with the ability to become successful medications. The methods and research presented in this paper demonstrate the distinctive advantages of this approach and its high throughput performance in drug development. Top searched compounds by a graph neural network algorithm of the deep-learning module of DeepChem library fit in the active region of target COX-2 and block the active site computationally. Many highly predicted drugs are known COX-2 inhibitors, which confirms the robustness of the present methodology. Besides known COX-2 inhibitors, vismodegib, an anticancer medication, has demonstrated the

potential to inhibit COX-2. Furthermore, the experimental evaluation of COX-2 inhibitory activity of COX-2 in RBL-2H3 cells was in correlation with results from deep-learning and molecular docking analyses. Therefore, it is concluded that vismodegib can be considered a novel COX-2 inhibitor and that deep-learning-based drug repositioning can be a promising approach for drug repurposing and drug screening in novel drug development for COX-2 inhibitors and a variety of other targets.

## METHODOLOGY

### COX-2 Data Sets and FDA-Approved Drug Library.

COX-2 active and decoy data sets were downloaded from the DUD-E Web site (<https://dude.docking.org/>). Active and decoy data sets were composed of 435 and 23,150 compounds, respectively. All molecules were expressed as canonicalized SMILES strings with DUD-E and ChEMBL ID numbers. Compounds were labeled as active and decoy in legend. FDA-approved drug library was obtained from the Web site of Selleck Chemicals (<https://www.selleckchem.com>). Drug molecules, composed of 3105 compounds, were expressed as SDF (structure-data file) and converted to SMILES strings using RDKit.

**Molecular Descriptor Generation Using RDKit.** To generate molecular descriptors from compounds, RDKit was used. RDKit is an open-source, high-performance cheminformatics, and machine-learning toolkit written in Python (<https://www.rdkit.org>). The toolkit includes the functionality for molecular descriptor calculations, chemical feature generation, and chemical data visualization.

**Deep-Learning Architecture.** The COX-2 active and decoy data sets were divided into training, validation, and test sets at the ratio of 8:1:1. Deep-learning analysis was carried out using the GraphConvMol model in DeepChem (<https://deepchem.io/models>). The GraphConvMol, a graph convolutional neural network, enables the model to learn features from graph-structured input data such as molecular graphs. Briefly, the architecture of GraphConvMol is as follows: first, the model preprocesses molecular structures into graphs, where atoms and bonds are nodes and edges, respectively. Next, a set of graph convolutional layers is stacked to extract hierarchical features from the molecular graphs. These layers consist of trainable parameters with different weights that adjust and optimize the learning process for the model to accurately capture the molecular structures' characteristics. During the training phase, the model minimizes the loss function with respect to the input molecular data sets and, in turn, optimizes the weights of the convolutional layers using backpropagation. The model aims to predict the properties of a given molecule, including solubility, bioactivity, and toxicity, based on the molecular structures.

**COX-2 Structure Retrieval.** The 3D structure of human COX-2 protein (PDB ID: 5KIR with 2.70 Å resolution) was obtained from the protein data bank (PDB) (<https://www.rcsb.org>), and further its energy minimization was carried out using UCSF Chimera.<sup>37</sup> The COX-2 protein, which is made up of  $\alpha$ -helices,  $\beta$ -sheets, coils, and turns, was subjected to a quantitative protein structure analysis using the internet server VADAR 1.8 (<http://vadar.wishartlab.com/>). Additionally, the Ramachandran graphs were computed using the Discovery Studio Client.<sup>38</sup>

**Prediction of Active Binding Site.** The position of a ligand in the protein's holo-structure most likely determines the binding pocket of the protein.<sup>39</sup> The complex of COX-2 and inhibitor, Vioxx, was retrieved from PDB (PDB ID: 5KIR). The interacting amino acids were selected using the ligand interaction approach of Discovery Studio for the accuracy of binding site generation. Furthermore, the cocrystallized ligand was selected and the binding sphere was constructed by the current selection technique in the defined binding site window of Discovery Studio. Consequently, the binding sphere was contracted with restrictions on selected amino acids.

**Molecular Docking.** Molecular docking is the most widely used method for evaluating the interactions and conformations of ligands with target proteins.<sup>40</sup> It anticipates the association strength or binding affinity between two molecules based on preferred orientation by using scoring algorithms.<sup>30</sup> The water molecules and cocrystallized ligand molecules were removed from the protein, and the hydrogens were added to the protein by Discovery Studio's protein preparation module. The ligand preparations were also carried out for reference and candidate compounds in which tautomers were generated, ionization was subjected to change, and bad valences were fixed by Discovery Studio's ligand preparation module. The CDOCKER module of Discovery Studio was employed to perform molecular docking of ligands against COX-2 with default orientations and conformation. The lowest binding interaction energy values (kcal/mol) were utilized to estimate the best-docked complexes.

**Binding Interaction Analysis.** The ligand docked complexes were analyzed graphically in three dimensions (3D) using UCSF Chimera 1.10.1<sup>37</sup> and Discovery Studio Client to study the interactions with the COX-2 protein.

**Experimental Reagents and Cell culture.** Celecoxib, ibuprofen, vismodegib, phorbol 12-myristate 13-acetate (PMA), and A23187, a calcium ionophore, were purchased from Sigma-Aldrich (St. Louis, MO, USA). Rat basophilic leukemia (RBL-2H3) cells were obtained from the Korea cell line bank (KCLB), KCLB cat #22256. RBL-2H3 cells were maintained in medium RPMI 1640 (RPMI 1640; Hyclon Laboratories) containing 10% heat-inactivated fetal bovine serum and 100 U/mL penicillin-streptomycin (Gibco) at 37 °C, 5% CO<sub>2</sub>.

**PGE<sub>2</sub> Assays.** RBL-2H3 cells were pretreated with drugs for 24 h and then challenged with or without PMA/A23187 (1  $\mu$ g/mL) for 24 h. PGE<sub>2</sub> released into the culture media of RBL-2H3 was measured using enzyme-linked immunosorbent (ELISA) kits (R&D system, USA) according to the manufacturer's instructions.

**Statistical Analysis.** All values shown in the figures are expressed as the mean  $\pm$  SD obtained from at least three independent experiments. Statistical significance was analyzed by a two-tailed Student's *t* test. Data with values of *p* < 0.05

were considered statistically significant. Double (\*\*) marks represent the statistical significance in *p* < 0.01.

## ■ ASSOCIATED CONTENT

### Data Availability Statement

The data that support the findings of this study are available from the corresponding author upon reasonable request.

## ■ AUTHOR INFORMATION

### Corresponding Author

Wanjoo Chun – Department of Pharmacology, Kangwon National University School of Medicine, Chuncheon 24341, Republic of Korea; [orcid.org/0000-0003-1984-3545](https://orcid.org/0000-0003-1984-3545); Phone: + 82-33-250-8853; Email: [wchun@kangwon.ac.kr](mailto:wchun@kangwon.ac.kr)

### Authors

Muhammad Yasir – Department of Pharmacology, Kangwon National University School of Medicine, Chuncheon 24341, Republic of Korea

Jinyoung Park – Department of Pharmacology, Kangwon National University School of Medicine, Chuncheon 24341, Republic of Korea

Eun-Taek Han – Department of Medical Environmental Biology and Tropical Medicine, Kangwon National University School of Medicine, Chuncheon 24341, Republic of Korea

Won Sun Park – Department of Physiology, Kangwon National University School of Medicine, Chuncheon 24341, Republic of Korea

Jun-Hee Han – Department of Medical Environmental Biology and Tropical Medicine, Kangwon National University School of Medicine, Chuncheon 24341, Republic of Korea

Yong-Soo Kwon – College of Pharmacy, Kangwon National University School of Medicine, Chuncheon 24341, Republic of Korea

Hee-Jae Lee – Department of Pharmacology, Kangwon National University School of Medicine, Chuncheon 24341, Republic of Korea

Complete contact information is available at:

<https://pubs.acs.org/10.1021/acsomega.3c05425>

### Author Contributions

M.Y. and J.P. were involved in the experimental operation and data analysis. E.-T.H., W.S.P., and J.-H.H. were involved in data curation and in the methodology. Y.-S.K. was involved in the project administration. W.C. was involved in the conceptualization, writing, reviewing, and editing of the manuscript. H.-J.L. and W.C. confirmed the authenticity of all the raw data. All authors have read and approved the final manuscript.

### Funding

Korea NRF 2021-R1A4A1031574

### Notes

The authors declare no competing financial interest.

## ■ ACKNOWLEDGMENTS

This work was supported by the National Research Foundation of Korea (NRF) grant funded by the Korea government [2021-R1A4A1031574].

## REFERENCES

- (1) Jourdan, J. P.; Bureau, R.; Rochais, C.; Dallemagne, P. Drug repositioning: a brief overview. *J. Pharm. Pharmacol.* **2020**, *72* (9), 1145–1151.
- (2) Parvathaneni, V.; Kulkarni, N. S.; Muth, A.; Gupta, V. J. D.; D, T. Drug repurposing: a promising tool to accelerate the drug discovery process. *Drug Discov. Today* **2019**, *24* (10), 2076–2085.
- (3) Zhao, L.; Ciallella, H. L.; Aleksunes, L. M.; Zhu, H. J. D. Advancing computer-aided drug discovery (CADD) by big data and data-driven machine learning modeling. *Drug Discov. Today* **2020**, *25* (9), 1624–1638.
- (4) Ramsay, R. R.; Popovic-Nikolic, M. R.; Nikolic, K.; Uliassi, E.; Bolognesi, M. L. J. C. A perspective on multi-target drug discovery and design for complex diseases. *Clin. Transl. Med.* **2018**, *7* (1), 3 DOI: 10.1186/s40169-017-0181-2.
- (5) Maia, E. H. B.; Assis, L. C.; De Oliveira, T. A.; Da Silva, A. M.; Taranto, A. G. Structure-based virtual screening: from classical to artificial intelligence. *Front. Chem.* **2020**, *8*, 343 DOI: 10.3389/fchem.2020.00343.
- (6) Zhong, S.; Zhang, K.; Bagheri, M.; Burken, J. G.; Gu, A.; Li, B.; Ma, X.; Marrone, B. L.; Ren, Z. J.; Schrier, J. J. E. S. Machine learning: new ideas and tools in environmental science and engineering. *Environ. Sci. Technol.* **2021**, *55* (19), 12741–12754.
- (7) Howard, J. J. A.; J, O. I. M. Artificial intelligence: Implications for the future of work. *Am. J. Ind. Med.* **2019**, *62* (11), 917–926.
- (8) Dara, S.; Dhamecherla, S.; Jadav, S. S.; Babu, C. M.; Ahsan, M. J. Machine Learning in Drug Discovery: A Review. *Artif. Intell. Rev.* **2022**, *55* (3), 1947–1999.
- (9) Nag, S.; Baidya, A. T. K.; Mandal, A.; Mathew, A. T.; Das, B.; Devi, B.; Kumar, R. Deep learning tools for advancing drug discovery and development. *3 Biotech* **2022**, *12* (5), 110 DOI: 10.1007/s13205-022-03165-8.
- (10) Jordan, M. I.; Mitchell, T. M. J. S. Machine learning: Trends, perspectives, and prospects. *Science* **2015**, *349* (6245), 255–260.
- (11) Wei, J.; Chu, X.; Sun, X. Y.; Xu, K.; Deng, H. X.; Chen, J.; Wei, Z.; Lei, M. J. I. Machine learning in materials science *InfoMat.* **2019**, *1* (3), 338–358 DOI: 10.1002/inf2.12028.
- (12) Stephenson, N.; Shane, E.; Chase, J.; Rowland, J.; Ries, D.; Justice, N.; Zhang, J.; Chan, L.; Cao, R. J. C.; D, M. Survey of machine learning techniques in drug discovery. *Molecules* **2019**, *20* (3), 185–193.
- (13) Miller, S. B. In Prostaglandins in health and disease: an overview, *Seminars in arthritis and rheumatism*; Elsevier: 2006; 37–49.
- (14) Balistreri, C. R. J. E., Inflammation; Diseases, C. I., *Eicosanoids in Tissue Regeneration, Repair and Injury Healing*; Nova Science Publishers Inc. 2015, 175.
- (15) Nanda, N.; Dhawan, D. K. Role of cyclooxygenase-2 in colorectal cancer. *Front. Biosci. (Landmark Ed)* **2020**, *26* (4), 706–716, DOI: 10.2741/4914.
- (16) Hidalgo-Estévez, A. M.; Stamatakis, K.; Jiménez-Martínez, M.; Lopez-Perez, R.; Fresno, M. J. F.; I, P. Cyclooxygenase 2-regulated genes an alternative avenue to the development of new therapeutic drugs for colorectal cancer. *Front. Pharmacol.* **2020**, *11*, 533.
- (17) Aparicio Gallego, G.; Díaz Prado, S.; Jimenez Fonseca, P.; García Campelo, R.; Cassinello Espinosa, J.; Antón Aparicio, L. M. J. C.; Oncology, T. Cyclooxygenase-2 (COX-2): a molecular target in prostate cancer. *Clin. Transl. Oncol.* **2007**, *9*, 694–702.
- (18) Luo, C.; Urgard, E.; Voorder, T.; Metspalu, A. J. M. H. The role of COX-2 and Nrf2/ARE in anti-inflammation and antioxidative stress: Aging and anti-aging. *Med. Hypotheses* **2011**, *77* (2), 174–178.
- (19) Amer, M.; Bead, V. R.; Bathon, J.; Blumenthal, R. S.; Edwards, D. N. J. C.; I, R. Use of nonsteroidal anti-inflammatory drugs in patients with cardiovascular disease: a cautionary tale. *Cardiol. Rev.* **2010**, *18* (4), 204–212.
- (20) Mysinger, M. M.; Carchia, M.; Irwin, J. J.; Shoichet, B. K. J. J.; O, M. C. Directory of useful decoys, enhanced (DUD-E): better ligands and decoys for better benchmarking. *J. Med. Chem.* **2012**, *55* (14), 6582–6594.
- (21) Zhang, Y.; Vass, M.; Shi, D.; Abualrous, E.; Chambers, J. M.; Chopra, N.; Higgs, C.; Kasavajhala, K.; Li, H.; Nandekar, P. J. J. O. C. I. Benchmarking refined and unrefined AlphaFold2 structures for hit discovery. *J. Chem. Inf. Model.* **2023**, *63* (6), 1656–1667.
- (22) Sabe, V. T.; Ntombela, T.; Jhamba, L. A.; Maguire, G. E. M.; Govender, T.; Naicker, T.; Kruger, H. G. Current trends in computer aided drug design and a highlight of drugs discovered via computational techniques: A review. *Eur. J. Med. Chem.* **2021**, *224*, No. 113705.
- (23) Minnich, A. J.; McLoughlin, K.; Tse, M.; Deng, J.; Weber, A.; Murad, N.; Madej, B. D.; Ramsundar, B.; Rush, T.; Calad-Thomson, S. J. J. O. AMPL: a data-driven modeling pipeline for drug discovery. *J. Chem. Inf. Model.* **2020**, *60* (4), 1955–1968.
- (24) Ramsundar, B.; Eastman, P.; Walters, P.; Pande, V. *Deep learning for the life sciences: applying deep learning to genomics, microscopy, drug discovery, and more*; "O'Reilly Media, Inc.": 2019.
- (25) Grebner, C.; Matter, H.; Kofink, D.; Wenzel, J.; Schmidt, F.; Hessler, G. J. C. Application of deep neural network models in drug discovery programs. *ChemMedChem* **2021**, *16* (24), 3772–3786.
- (26) Grebner, C.; Matter, H.; Hessler, G. J. A. I. I. D. D. Artificial intelligence in compound design. *Methods Mol. Biol.* **2022**, 349–382.
- (27) Passarelli, A.; Galdo, G.; Aieta, M.; Fabrizio, T.; Villonio, A.; Conca, R. A. Vismodegib experience in elderly patients with basal cell carcinoma: case reports and review of the literature. *Int. J. Mol. Sci.* **2020**, *21* (22), 8596 DOI: 10.3390/ijms21228596.
- (28) Kandekar, S. G.; Singhal, M.; Sonaje, K. B.; Kalia, Y. N. J. E.; O O, D. D. Polymeric micelle nanocarriers for targeted epidermal delivery of the hedgehog pathway inhibitor vismodegib: Formulation development and cutaneous biodistribution in human skin. *Expert Opin. Drug Deliv.* **2019**, *16* (6), 667–674.
- (29) Sirois, J.; Sayasith, K.; Brown, K. A.; Stock, A. E.; Bouchard, N.; Doré, M. J. H.; R, U. Cyclooxygenase-2 and its role in ovulation: a 2004 account. *Hum. Reprod. Update* **2004**, *10* (5), 373–385.
- (30) Yasir, M.; Park, J.; Han, E.-T.; Park, W. S.; Han, J.-H.; Kwon, Y.-S.; Lee, H.-J.; Hassan, M.; Klodzowski, A.; Chun, W. J. M. Exploration of Flavonoids as Lead Compounds against Ewing Sarcoma through Molecular Docking, Pharmacogenomics Analysis, and Molecular Dynamics Simulations. *Molecules* **2023**, *28* (1), 414.
- (31) Orlando, B. J.; Malkowski, M. G. Crystal structure of rofecoxib bound to human cyclooxygenase-2. *Acta Crystallogr. Sect. F, Struct. Biol. Commun.* **2016**, *72* (Pt 10), 772–776.
- (32) Wu, Y.; Brooks, C. L., III Flexible CDOCKER: Hybrid Searching Algorithm and Scoring Function with Side Chain Conformational Entropy. *J. Chem. Inf. Model.* **2021**, *61* (11), 5535–5549.
- (33) Yasir, M.; Park, J.; Han, E.-T.; Park, W. S.; Han, J.-H.; Kwon, Y.-S.; Lee, H.-J.; Chun, W. Computational Exploration of Licorice for Lead Compounds against Plasmodium vivax Duffy Binding Protein Utilizing Molecular Docking and Molecular Dynamic Simulation. *Molecules* **2023**, *28* (8), 3358.
- (34) Park, J. Y.; Lee, H. J.; Han, E. T.; Han, J. H.; Park, W. S.; Kwon, Y. S.; Chun, W. Caffeic acid methyl ester inhibits mast cell activation through the suppression of MAPKs and NF- $\kappa$ B signaling in RBL-2H3 cells. *Heliyon* **2023**, *9* (6), No. e16529.
- (35) Park, J. Y.; Lee, H. J.; Han, E. T.; Han, J. H.; Park, W. S.; Kwon, Y. S.; Chun, W. 3,4,5-Trihydroxycinnamic acid suppresses phorbol-12-myristate-13-acetate and A23187-induced mast cell activation in RBL-2H3 cells. *Exp. Ther. Med.* **2023**, *25* (5), 227 DOI: 10.3892/etm.2023.11926.
- (36) Juhasz, M.; Marmur, E. S. J. J.; O, D. I. D. J. Systematic review of vismodegib toxicity profile in the treatment of advanced basal cell carcinomas compared to other systemic therapies in dermatology. *J. Drugs Dermatol.* **2014**, *13* (6), 729–733.
- (37) Pettersen, E. F.; Goddard, T. D.; Huang, C. C.; Couch, G. S.; Greenblatt, D. M.; Meng, E. C.; Ferrin, T. E. J. J.; O, C. C. UCSF Chimera—a visualization system for exploratory research and analysis. *J. Comput. Chem.* **2004**, *25* (13), 1605–1612.
- (38) Studio, D. J. A. *Discovery studio*. 2008.

(39) Hassan, M.; Yasir, M.; Shahzadi, S.; Kloczkowski, A. J. A. O. Exploration of Potential Ewing Sarcoma Drugs from FDA-Approved Pharmaceuticals through Computational Drug Repositioning, Pharmacogenomics, Molecular Docking, and MD Simulation Studies. *ACS Omega* **2022**, *7* (23), 19243–19260.

(40) Yasir, M.; Park, J.; Han, E.-T.; Park, W. S.; Han, J.-H.; Kwon, Y.-S.; Lee, H.-J.; Hassan, M.; Kloczkowski, A.; Chun, W. Investigation of Flavonoid Scaffolds as DAX1 Inhibitors against Ewing Sarcoma through Pharmacoinformatic and Dynamic Simulation Studies. *Int. J. Mol. Sci.* **2023**, *24* (11), 9332.